Earth and Planetary Magnetospheres

Amitava Bhattacharjee

Center for Heliophysics

Department of Astrophysical Sciences

Princeton Plasma Physics Laboratory

Princeton University

LWS Heliophysics Summer School, July 6-July 17, 2020

Acknowledgements

F. Bagenal, J. Dorelli, F. Toffoletto Lectures

K. Schrijver, Principles of Heliophysics, Chapters 4-6

Radiation Belts

The discovery of Earth's radiation belts
Van Allen (1958)

Pickering, Van Allen and Von Braun with Explorer 1

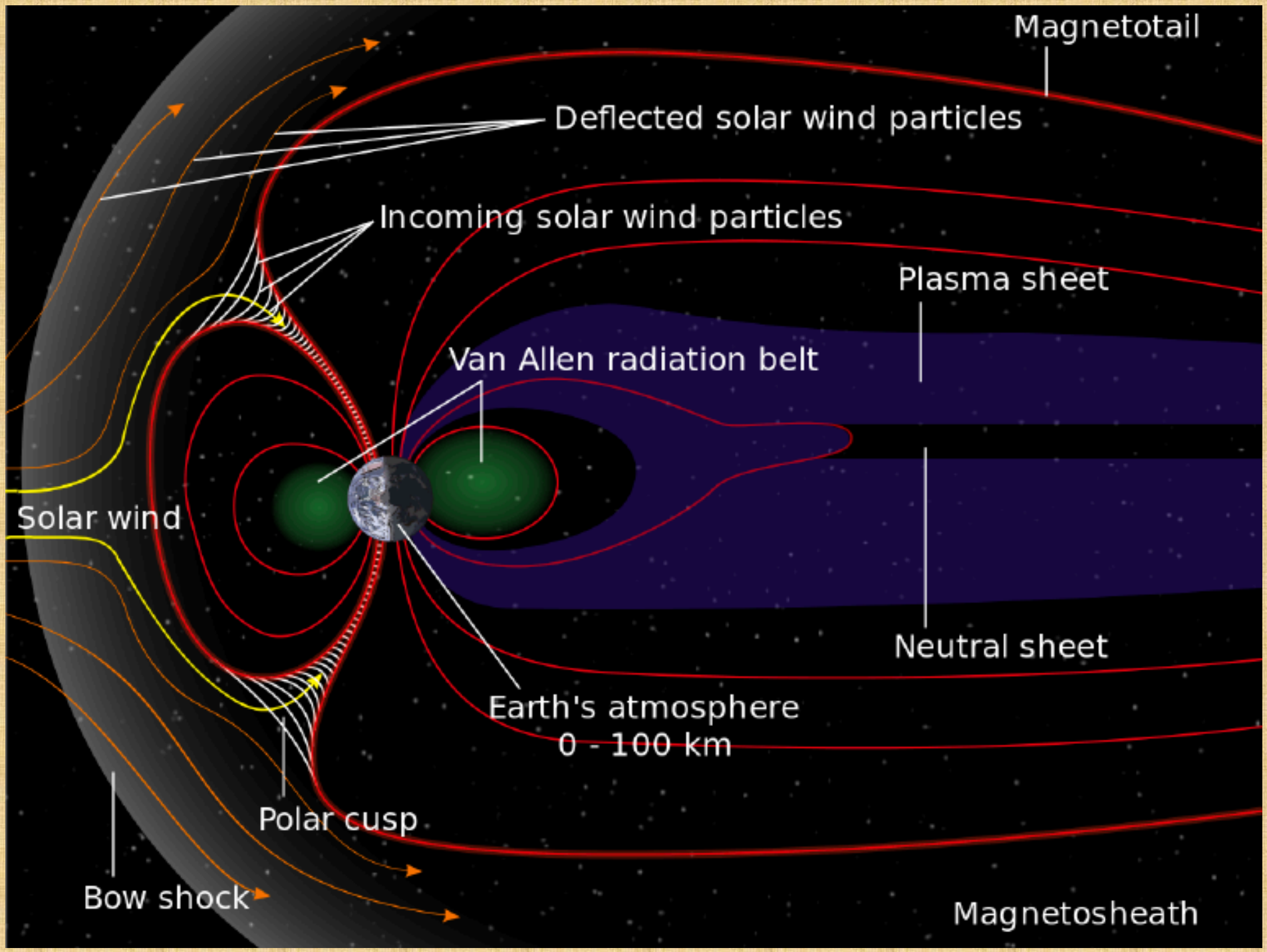
Magnetotail
Deflected solar wind particles
Incoming solar wind particles
Plasma sheet
Van Allen radiation belt
Solar wind
Neutral sheet
Earth's atmosphere
0 - 100 km
Polar cusp
Bow shock
Magnetosheath

Single-Particle Orbit Theory

Newton's law of motion for charged particles

$$m\frac{d\mathbf{v}}{dt} = q\left(\mathbf{E} + \mathbf{v}\times\mathbf{B}\right)$$

Guiding-Center: A very useful concept

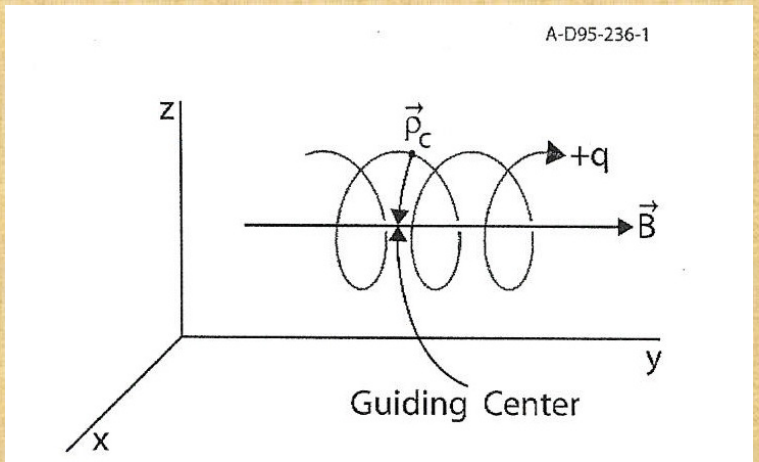

Single-Particle Orbit Theory

ExB Drift

$$m\frac{d\mathbf{v}}{dt} = q\left(\mathbf{E} + \mathbf{v}\times\mathbf{B}\right)$$

Consider $\mathbf{E} = const.,\ \mathbf{B} = const.$

The charged particles experience a drift velocity, perpendicular to both E and B, and independent of their charge and mass.

$$\mathbf{V_E} = \frac{\mathbf{E}\times\mathbf{B}}{B^2}$$

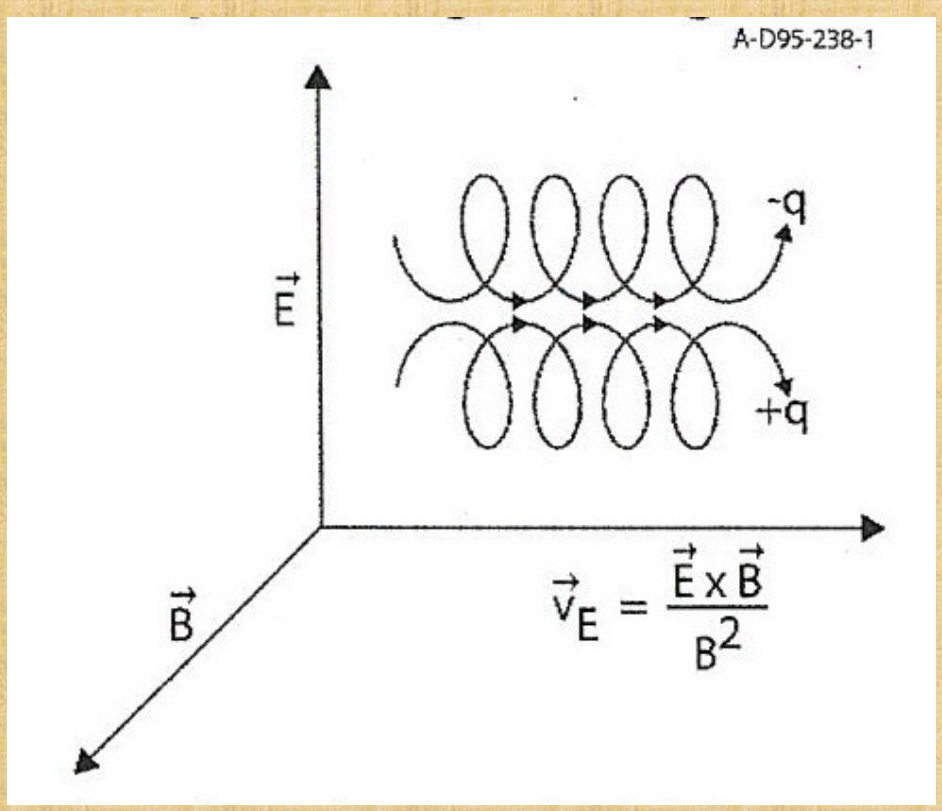
A-D95-238-1
$\vec{E}$
-q
+q
$\vec{B}$
$\vec{v}_E = \frac{\vec{E} \times \vec{B}}{B^2}$

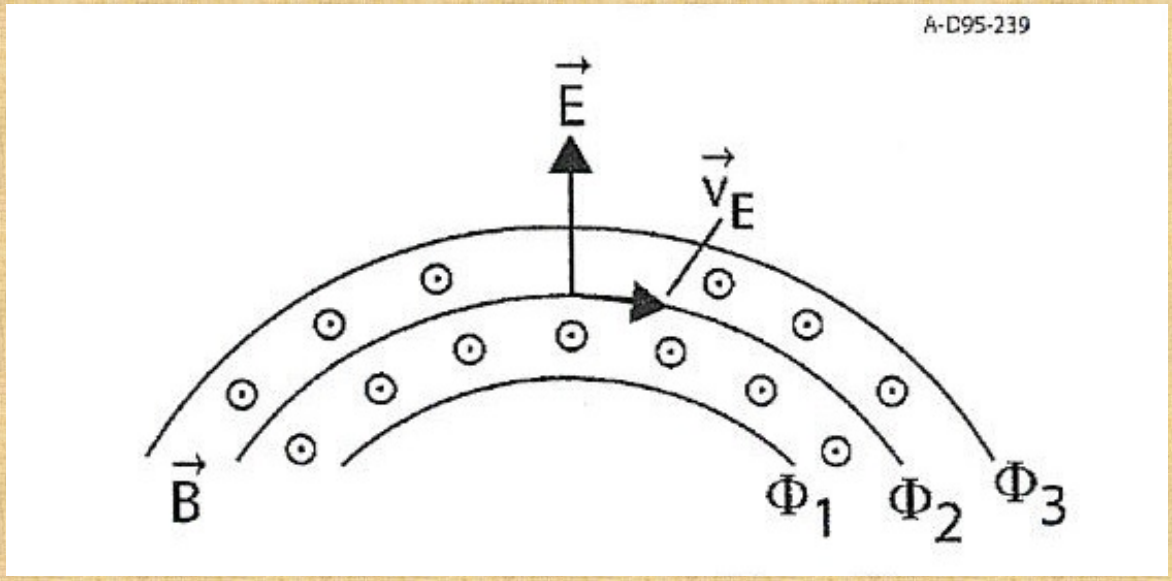
A-D95-239
$\vec{E}$
$\vec{v}_E$
$\vec{B}$
Φ_1
Φ_2
Φ_3

Gradient B drift

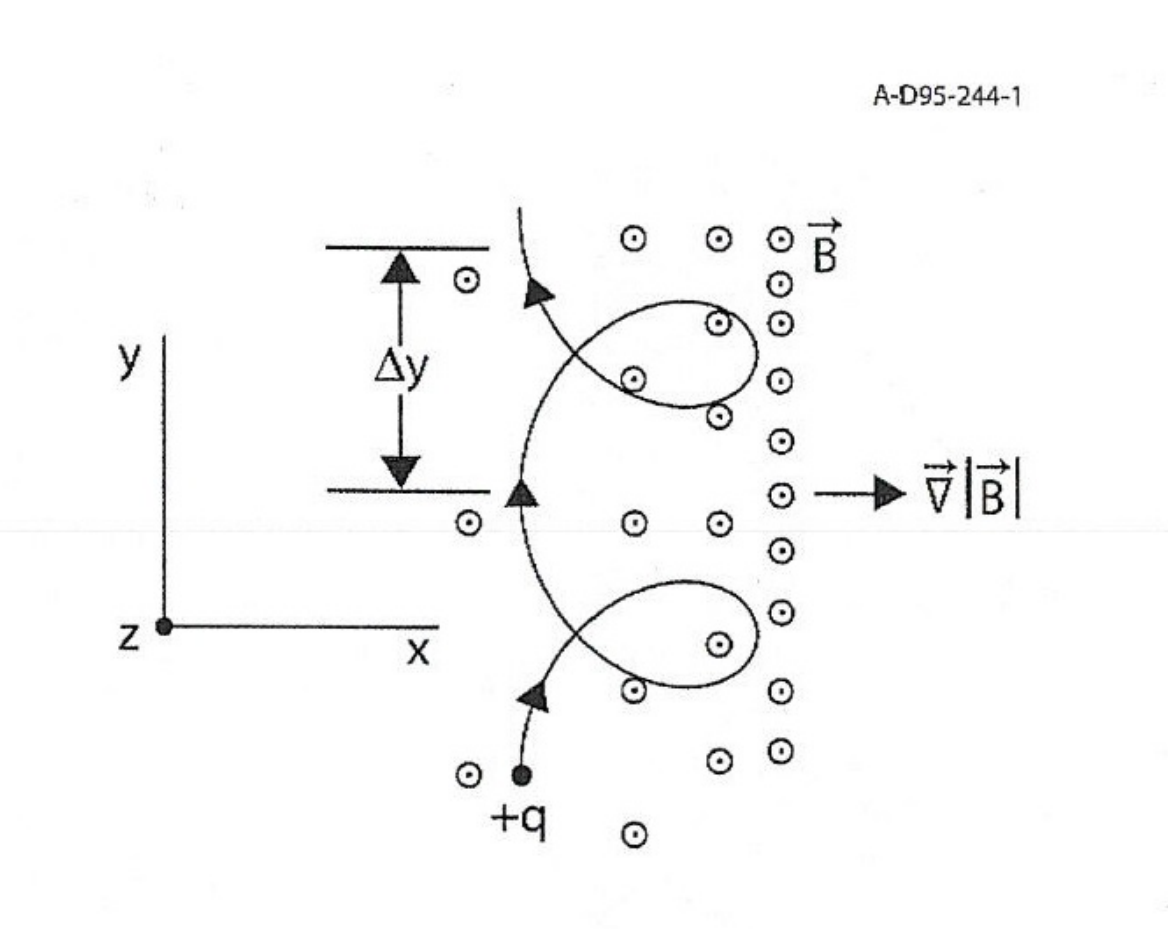

$$\mathbf{V_G} = \frac{w_\perp}{qB}\left(\frac{\mathbf{B}\times\nabla\mathbf{B}}{B^2}\right),$$

$$w_\perp = \frac{1}{2}\omega_c{}^2\rho_c{}^2$$

Curvature drift

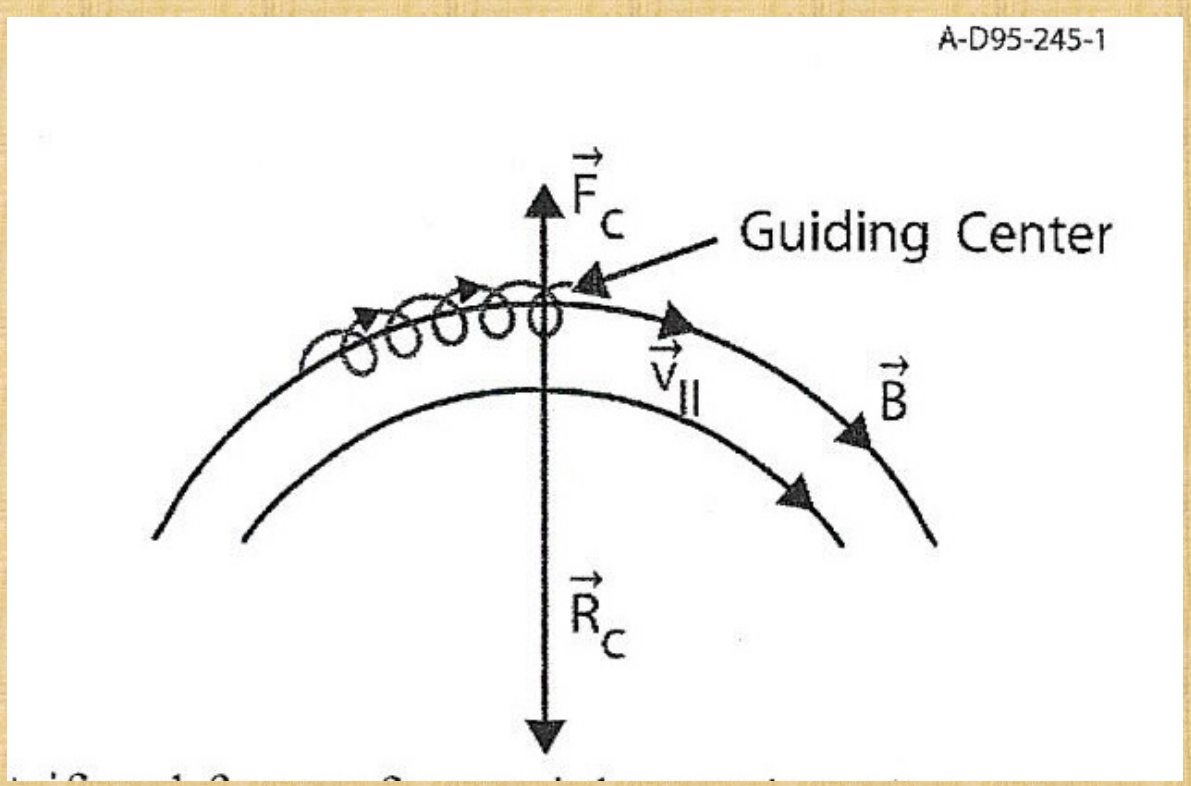

$$\mathbf{V}_C = \frac{2w_{||}}{qB^2}\left(\frac{\mathbf{R_C} \times \mathbf{B}}{{R_C}^2}\right),$$

$$w_{||} = \frac{1}{2} m {v_{||}}^2$$

The Ring Current in Earth's Magnetosphere: An Example

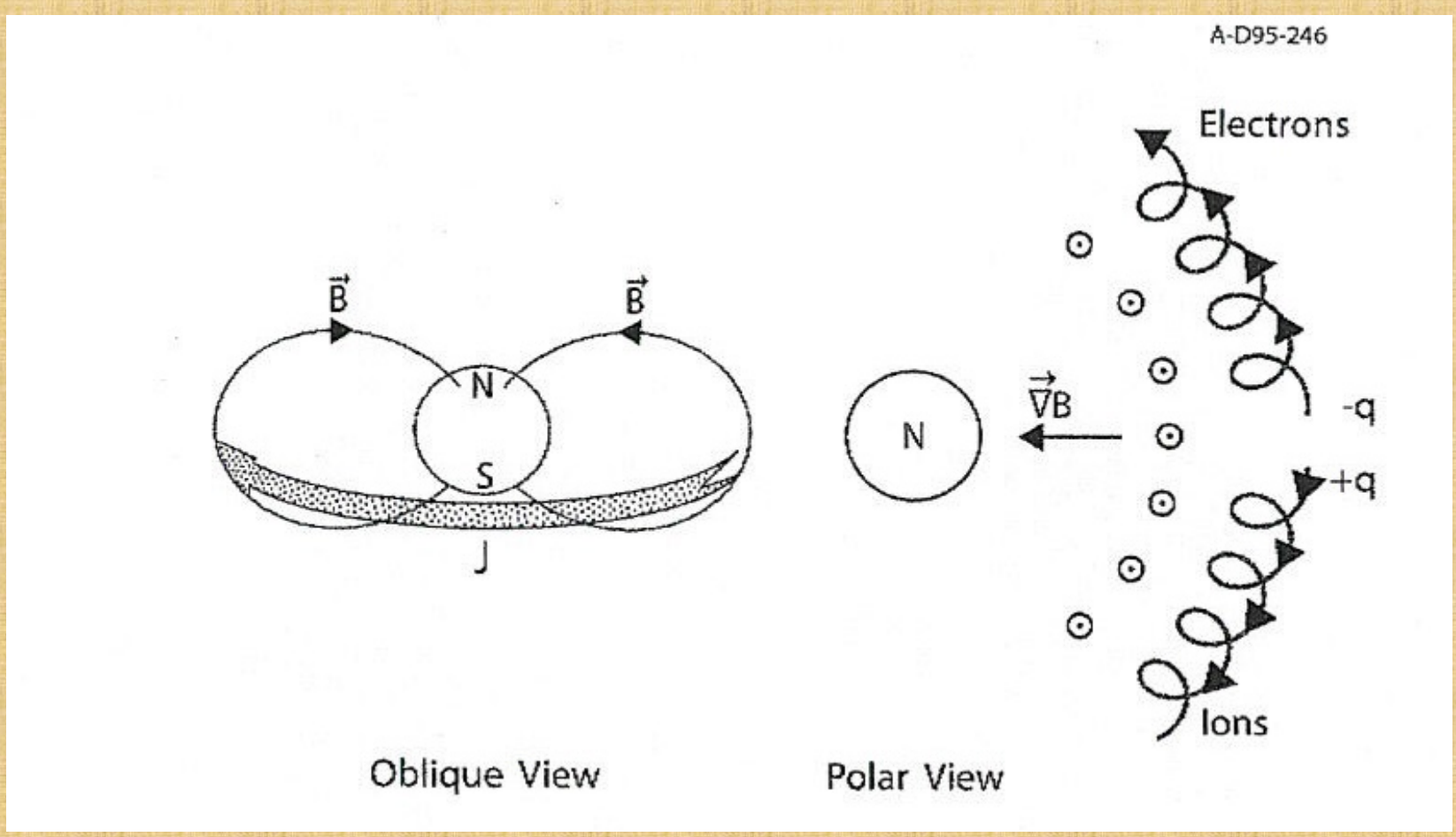

Adiabatic Invariants

Albert Einstein and the Adiabatic Pendulum (1911)

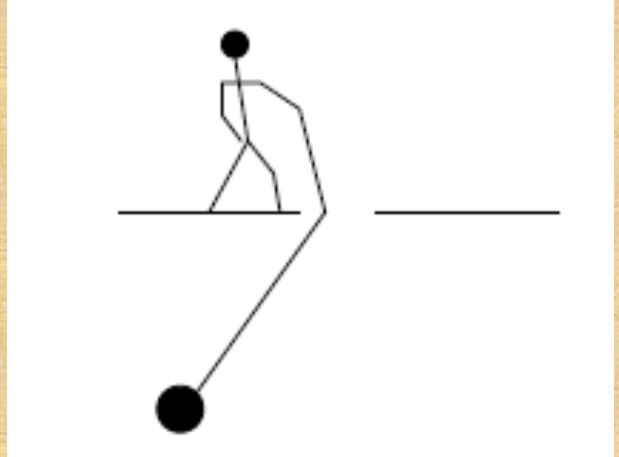

Einstein suggested that while both the energy E and the frequency ν change, the ratio E/ν remains approximately invariant.

Adiabatic Invariants

Harmonic oscillator

$$\frac{d^2x}{dt^2} + \omega^2(\varepsilon t)x = 0,\ \varepsilon << 1$$

The adiabatic invariant is

$$J = \oint p dq$$

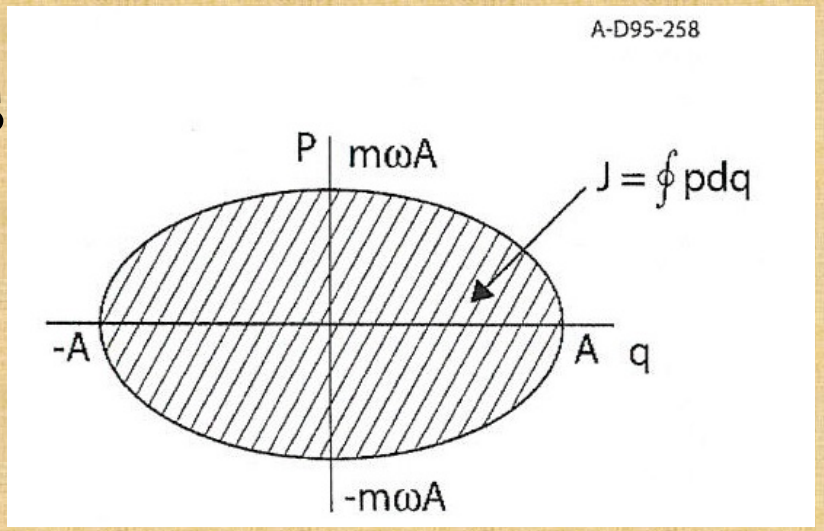

$$\Delta J / J \sim \exp(-c/\varepsilon)$$

Adiabatic Invariants

Three types of bounce motion

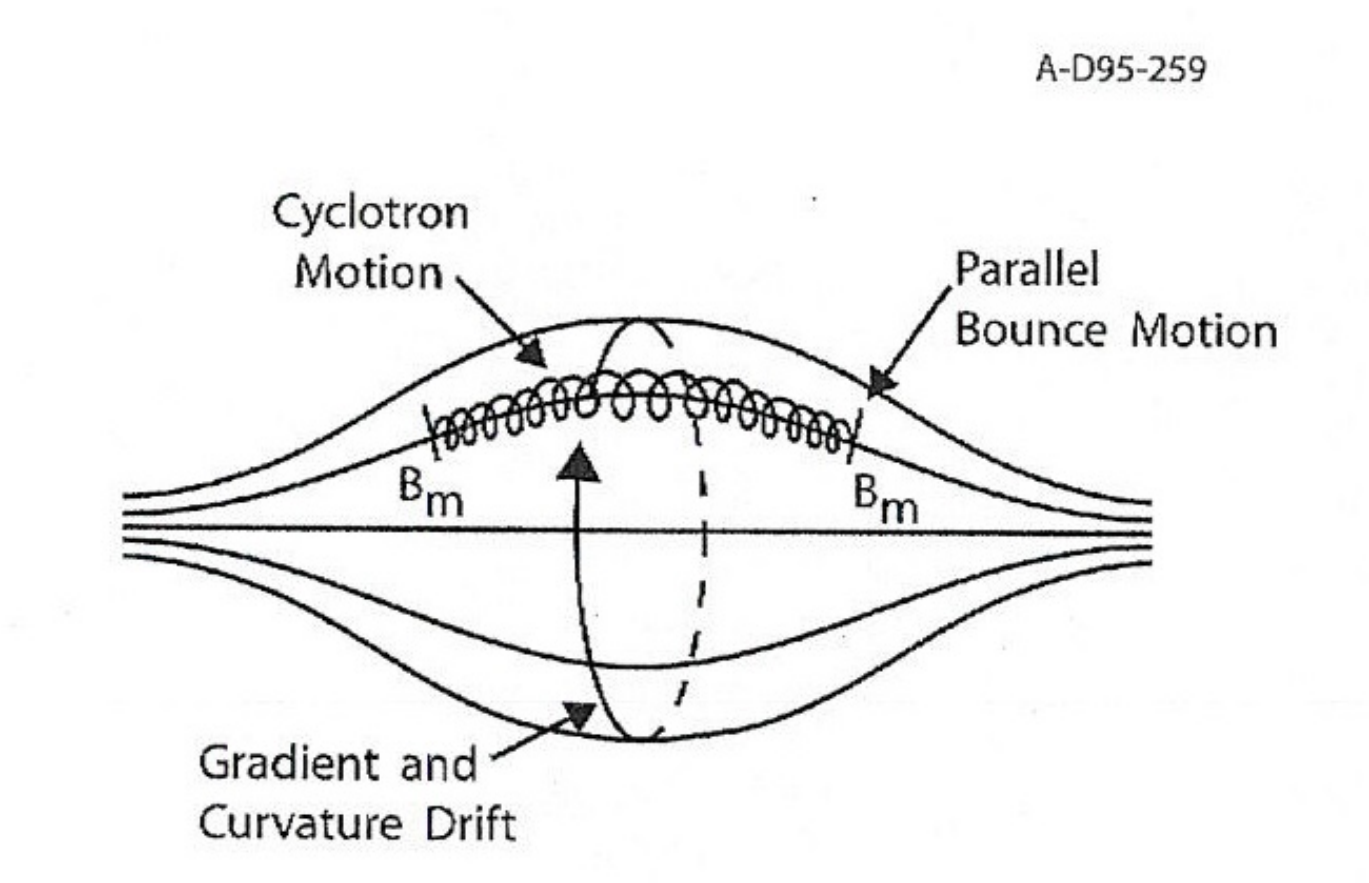

Adiabatic Invariants

Three types of bounce motion

First adiabatic invariant $\mu = w_{\perp} / B$

Second adiabatic invariant $J = m \oint v_{||} ds$

Third adiabatic invariant $\Phi = \pi R^2 B$

Adiabatic Invariants

Associated with each motion is a corresponding *adiabatic invariant:*

- Gyro: *M* *t~milliseconds*
- Bounce: *K* *t~0.1-1 sec*
- Drift: *L* *t~1-10 mins*

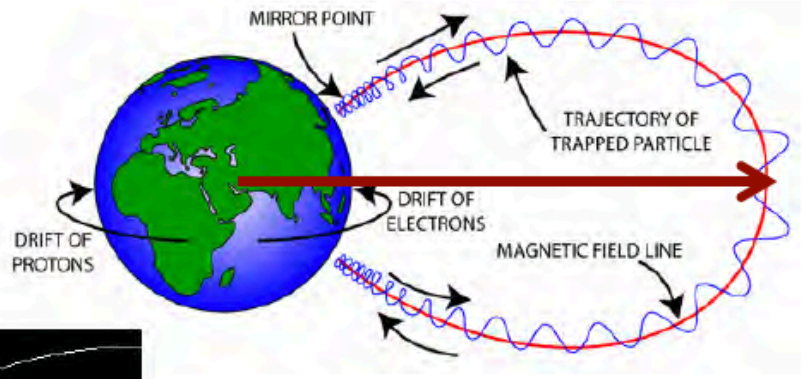

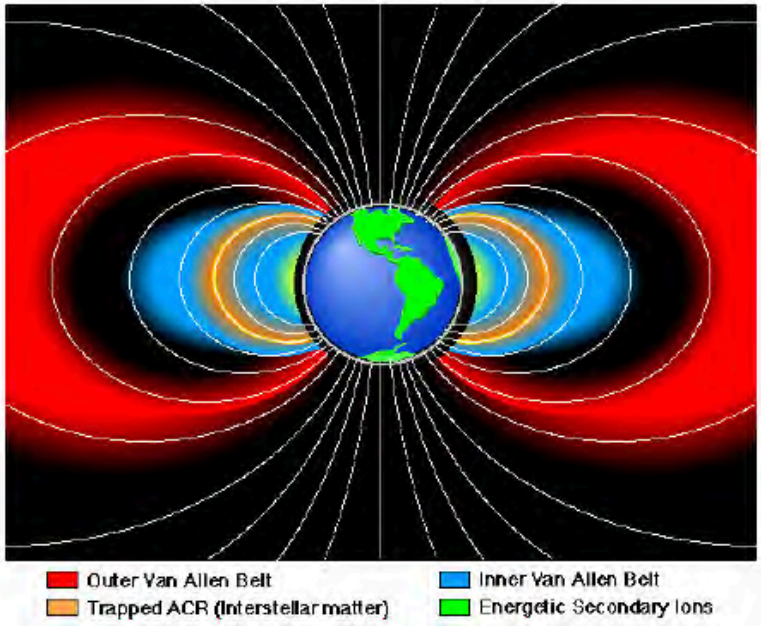

L: radial distance equator crossing in dipole field

If field guiding particles change slowly compared to characteristic motion - corresponding invariant is conserved.

RBSP, sources, and losses: the third radiation belt

Shortly after "First Light" for the Van Allen Probe's Relativistic Electron-Proton Telescope (REPT), an unusual radiation belt configuration was observed to form, consisting of three belts and two slot regions.

What combination of energization, transport, and loss could have led to this configuration?

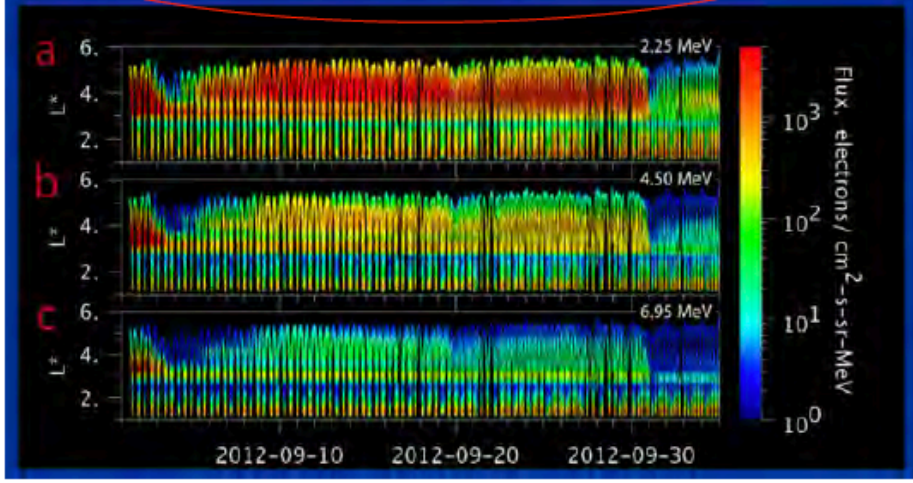

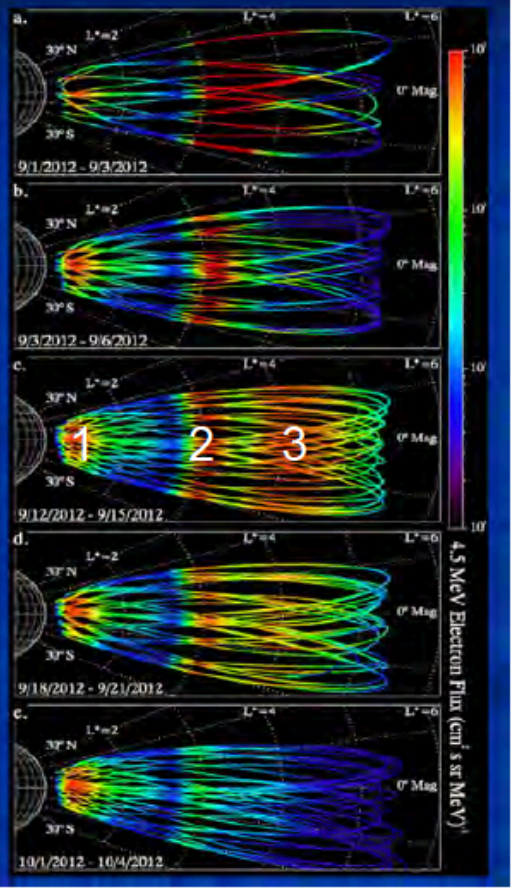

Magnetospheric current systems

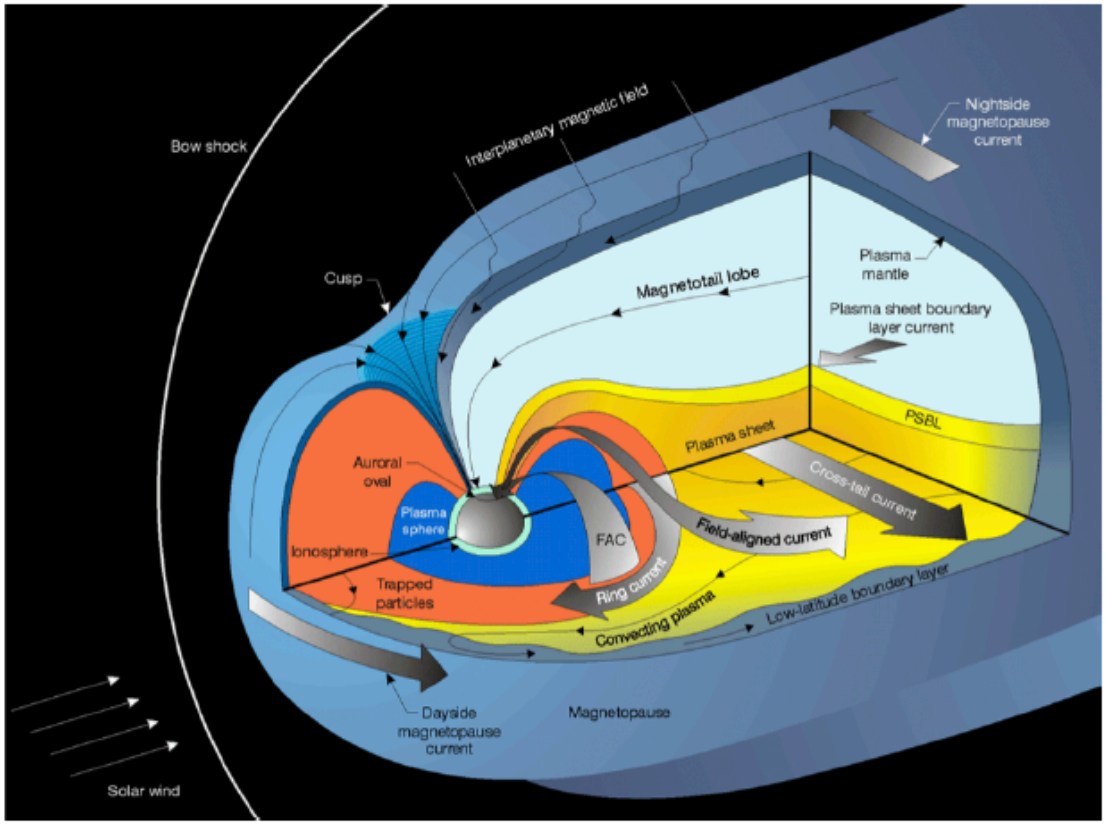

The Chapman-Ferraro Magnetosphere

S. Chapman

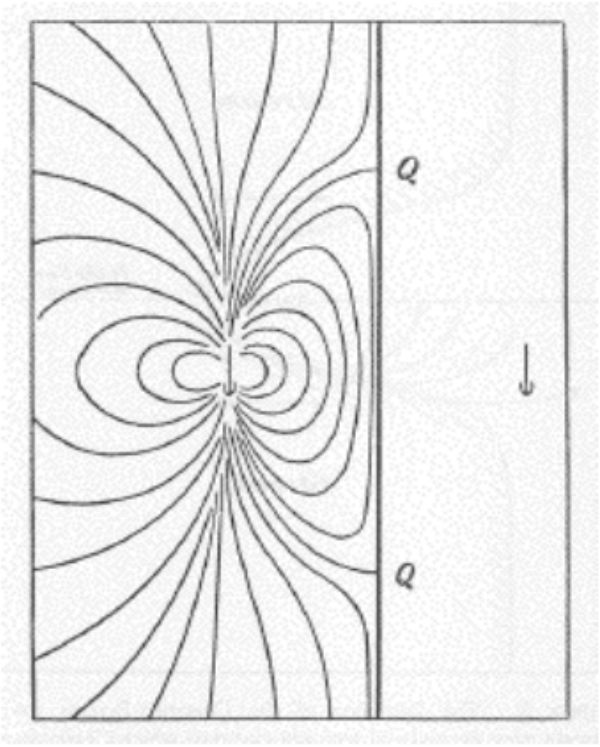

V. C. A.Ferraro

Chapman, S., and V. C. A. Ferraro, A new theory of magnetic storms, Terrest. Magnetism and Atmospheric Elec., 36, 171-186, 1931.

The Chapman-Ferraro Problem

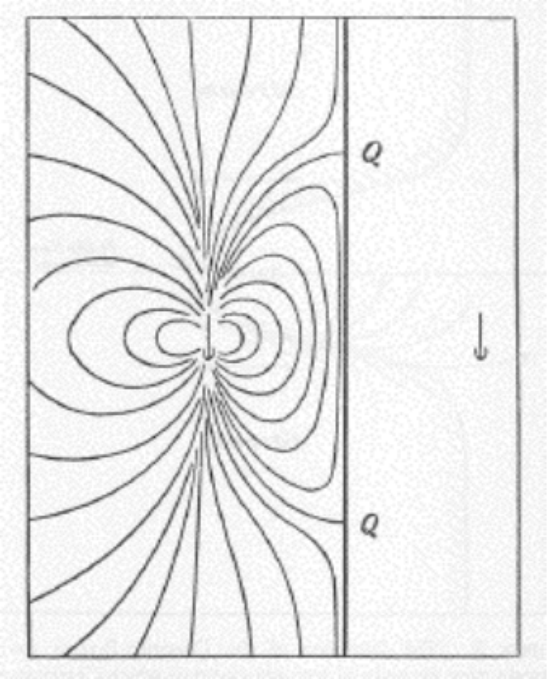

Find the surface that confines Earth's field and excludes the solar wind field.

If current density is confined to a set of pre-defined surfaces, one solves Laplace's equation for the magnetic potential:

$$B = -\nabla\Phi_M$$
$$\nabla^2\Phi_M = 0$$

We impose the boundary condition that the component of B normal to the pre-defined surfaces vanishes.

The Chapman-Ferraro Problem

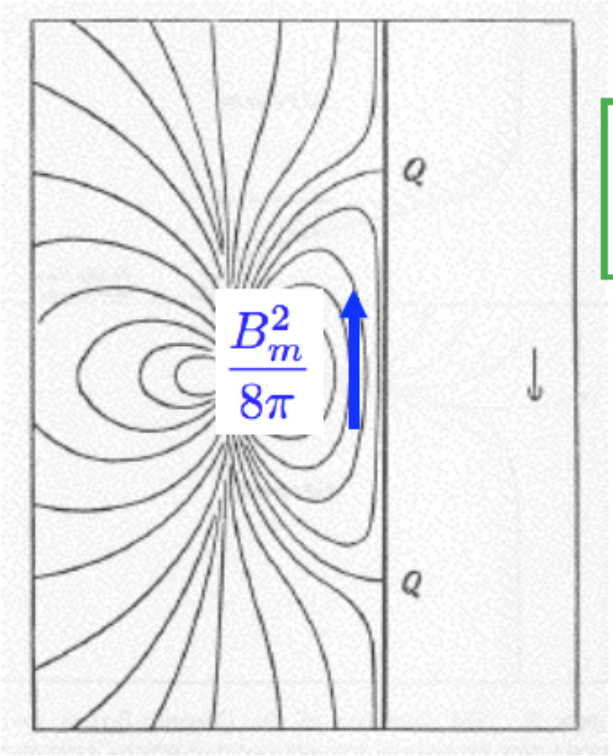

What about force balance?

$$\nabla \cdot \left[\rho \mathbf{V}\mathbf{V} + (p + \frac{B^2}{8\pi})\mathbf{I} - \frac{\mathbf{B}\mathbf{B}}{4\pi} \right] = 0$$

$\rho_{sw} V_{sw}^2$

Magnetic pressure in the magnetosphere balances solar wind dynamic pressure

Computing the shape of the magnetopause I: "Specular Reflection" off of a highly conducting bounday

$$\frac{B_t^2}{8\pi} = 2\rho_{sw} V_{sw}^2 \cos^2\theta$$

$$B_n = 0$$

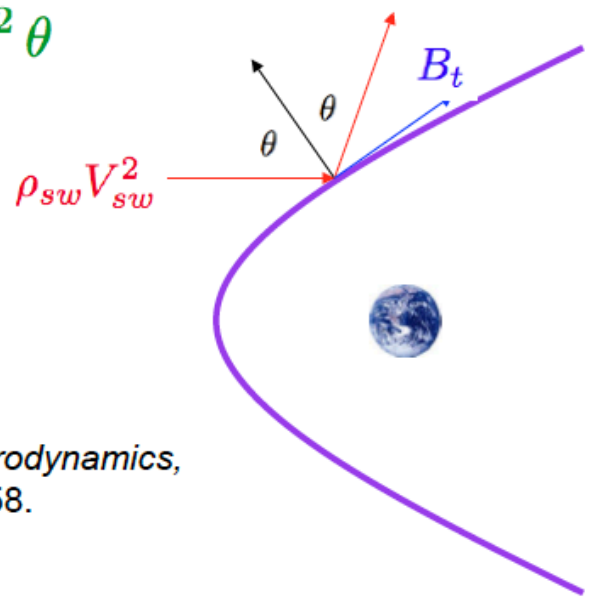

J. W. Dungey, *Cosmic Electrodynamics*, Cambridge U. Press, 1958.

A brute force solution….

$$\frac{B_t^2}{8\pi} = 2\rho_{sw} V_{sw}^2 \cos^2\theta$$

$$B_n = 0$$

1. Specify that magnetic field vanishes outside boundary surface S.
2. Parameterize the surface S (37 independent parameters in Midgley and Davis!).
3. Pressure balance relates surface current to the shape of the surface.
4. Spherical-harmonics expansion of surface current with coefficients chosen (by searching 37-dimensional parameter space) to cancel dipole outside surface.

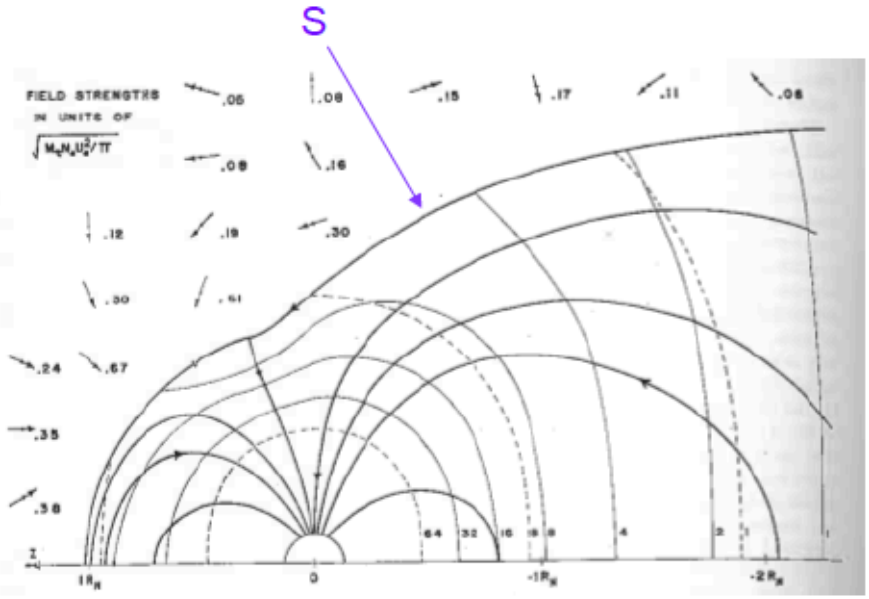

J. E. Midgley and L. Davis, *J. Geophys. Res.*, 68, 1963.

The structure of the magnetosheath

$$\frac{B_t^2}{8\pi} = K \rho_{sw} V_{sw}^2 \cos^2\theta$$

$$B_n = 0 \qquad K \approx 0.881$$

The "specular reflection" idea is not a very realistic model of the deflection of the solar wind around the magnetopause.

It turns out that gas dynamics (in which the magnetic field is neglected) does a pretty good job of describing the plasma flow in the magnetosheath.

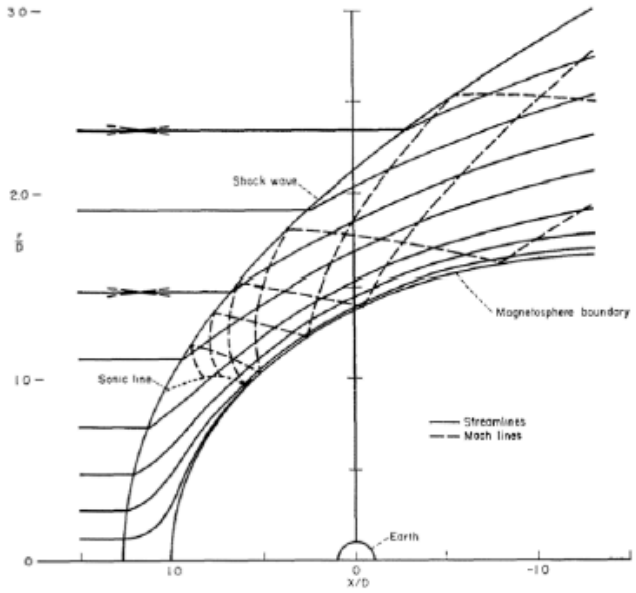

J. R. Spreiter, A. L. Summers and A. Y. Alksne, *Planet. Space Sci.*, 14, 1966.

Magnetosheath– Gasdynamic Aspects

- The energy of the solar wind is dominated by the flow
- The theoretical way to deal with this is to treat the flow as gasdynamic and to neglect the magnetic field.
  - Back in the 1960's, John Spreiter and colleagues converted an existing numerical code to describe the bow shock and magnetosheath. The code had been developed to treat the flow around missiles.
  - They assumed an axially symmetric shape for the magnetopause.
- Since the solar wind is supersonic, it forms a shock as it encounters the Earth's magnetosphere and slows down
  - The collision mean free path of the solar wind is of the order of ~10^6 R_E, the thickness of the bow shock is of the order of the ion gyroradius (~1000 km)

Bow shock stand-off distance

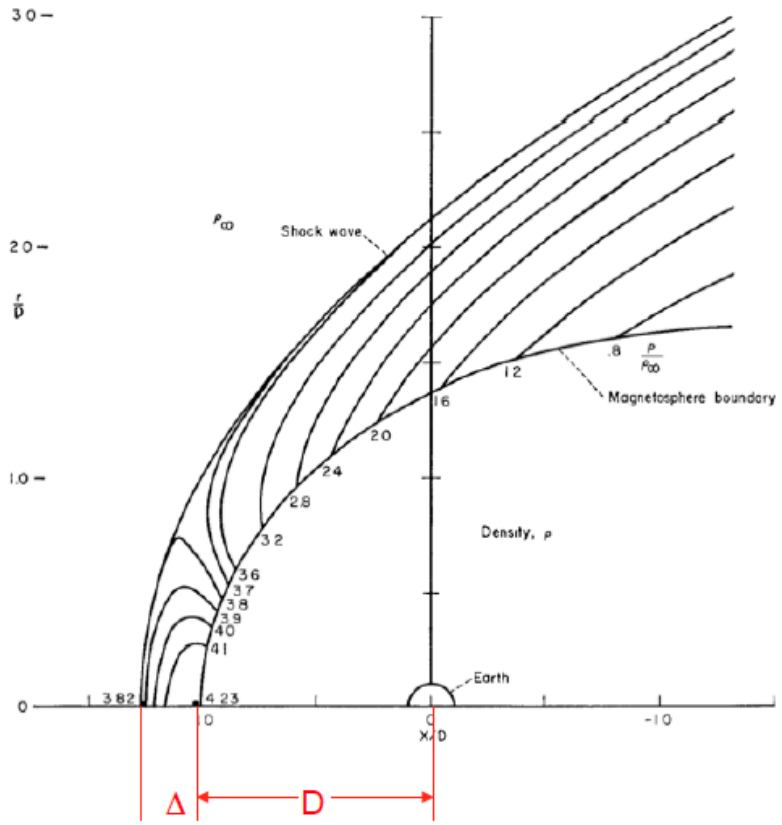

$$\frac{\rho_1}{\rho_\infty} = \frac{(\gamma+1)M_\infty^2}{(\gamma-1)M_\infty^2+2}$$

$$\frac{\Delta}{D} = 1.1\frac{\rho_\infty}{\rho_1}$$

This relationship breaks down when the upstream mach number approaches 1.

Pressure pileup at subsolar magnetopause

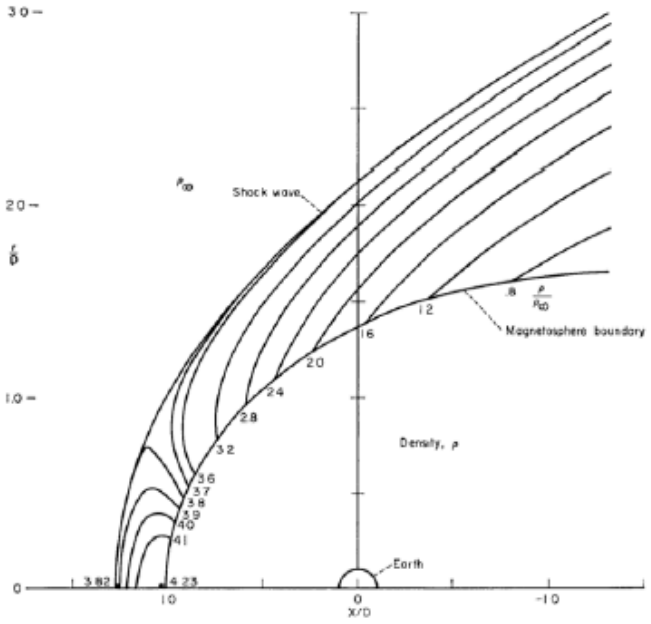

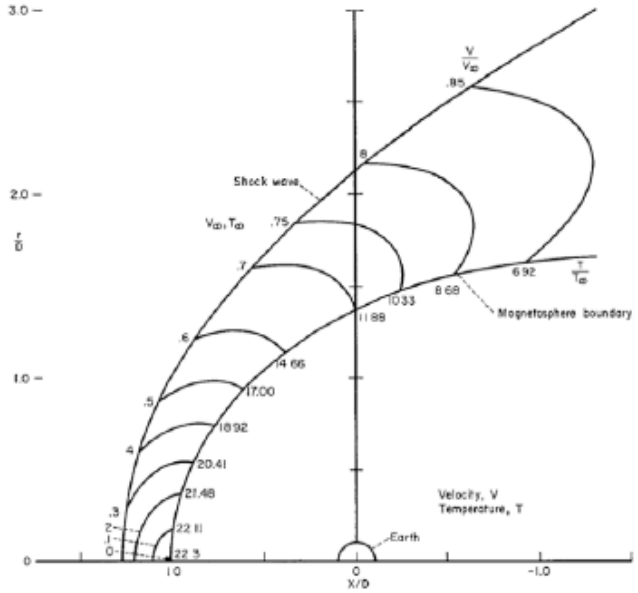

Pressure must increase as we approach the subsolar magnetopause (to divert the solar wind around the magnetopause).

What happens when we include the magnetic field?

What about the solar wind magnetic field?

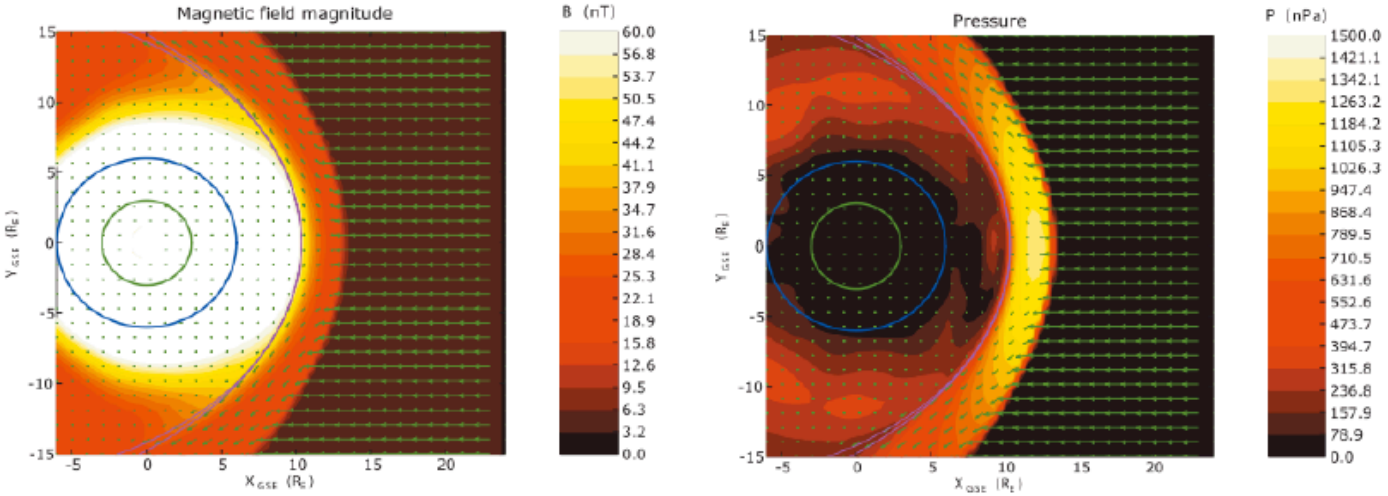

e.g., J. Dorelli and A. Bhattacharjee, *J. Geophys. Res.,* 114, 2009

Pressure (and density) decrease, while magnetic energy increases, as one approaches the subsolar magnetopause.

The "weak field" approximation breaks down when the solar wind magnetic field is included!

Magnetopause reconnection

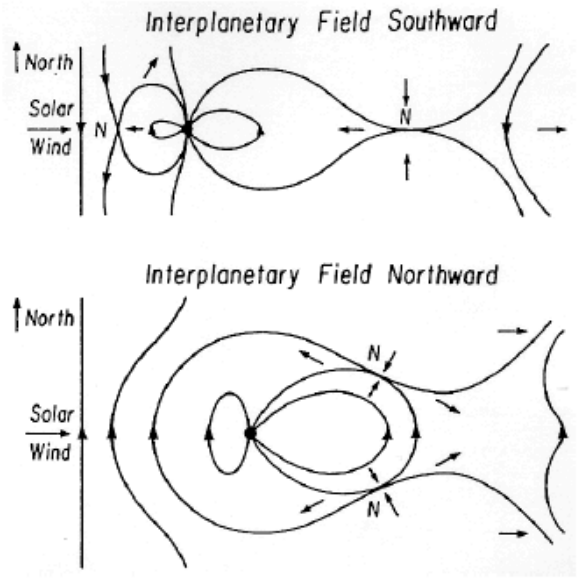

Dungey, J. W., PRL, 6, 47-48, 1961.

Dungey, J. W., in Geophysics: The Earth's Environment, eds., C. Dewitt *et al.*, 1963.

Breakdown of ideal MHD in a thin layer around the magnetopause implies that the solar wind field and plasma has access to the magnetosphere.

Magnetopause reconnection

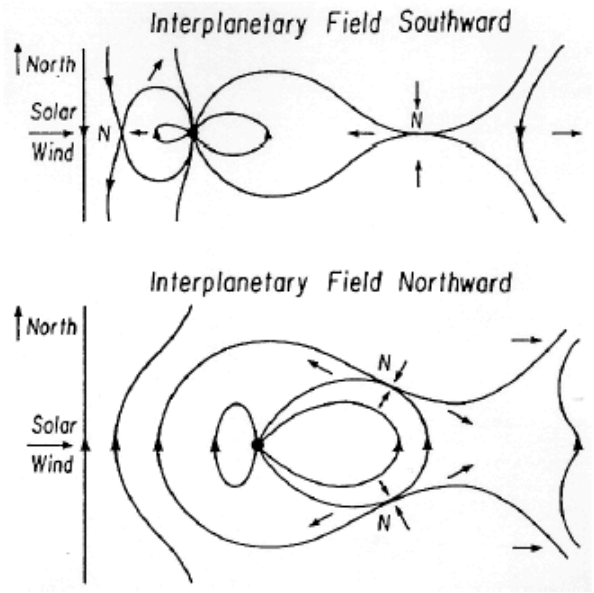

High geomagnetic activity
(magnetospheric storms and substorms)

Low geomagnetic activity
(fewer storms and substorms)

"Magnetopause phenomena are more complicated as a result of merging. This is why I no longer work on the magnetopause." -- *J. W. Dungey*

The auroral oval

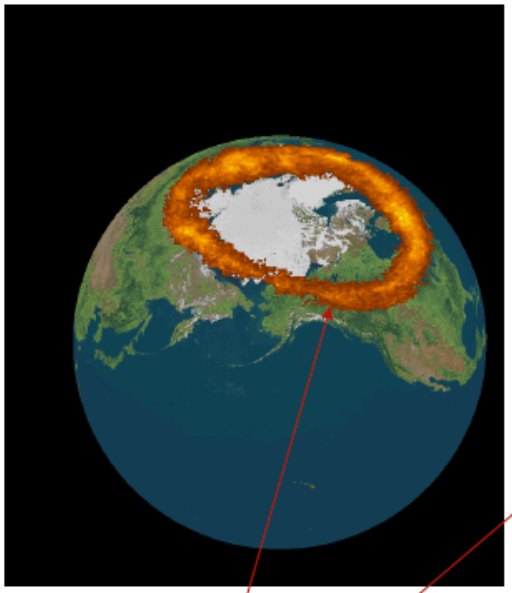

Polar VIS UV image of auroral oval (from http://eiger.physics.uiowa.edu/~vis/examples)

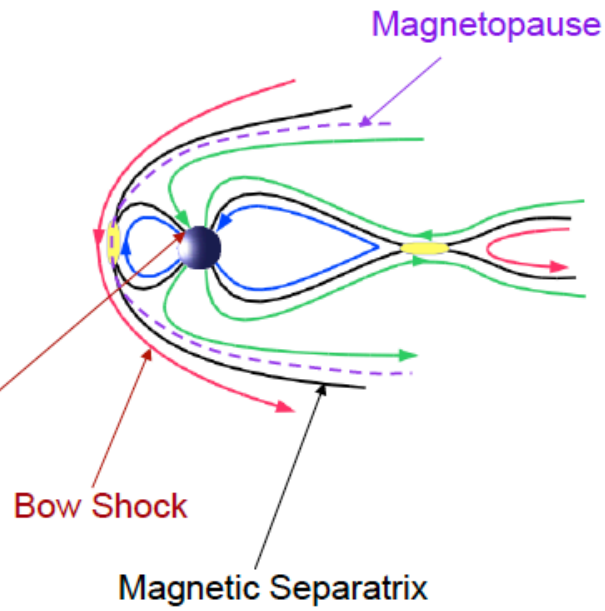

Auroral oval marks the boundary between open and closed field lines; the reconnection rate can be determined from radar observations of ionospheric convection (e.g., de la Beaujardiere *et al.*, J. Geophys. Res., 96, 13,907-13,912, 1991.).

Earth's magnetosphere features the interaction of collisionless, magnetized plasmas

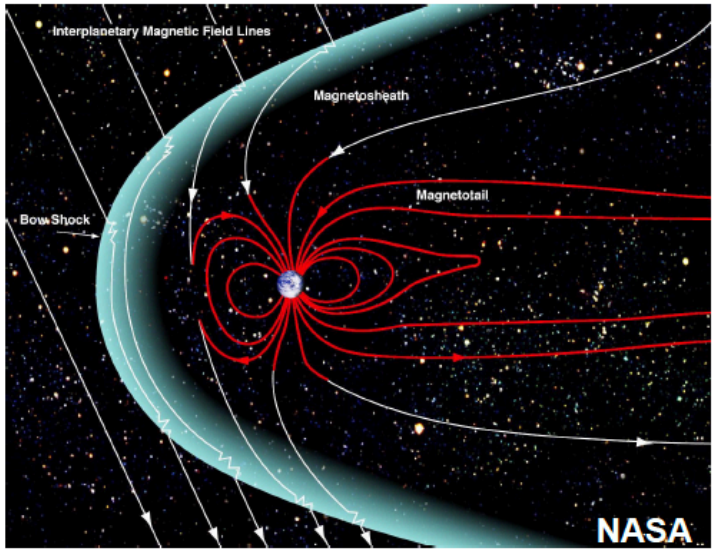

- The solar wind interaction stretches magnetic field lines into an extended tail
- Excess energy and magnetic flux are stored in the magnetotail

- The magnetotail can become unstable and explosively release stored energy in substorms
- Magnetospheric substorms energize particles and intensify the aurora

Simulation initial conditions

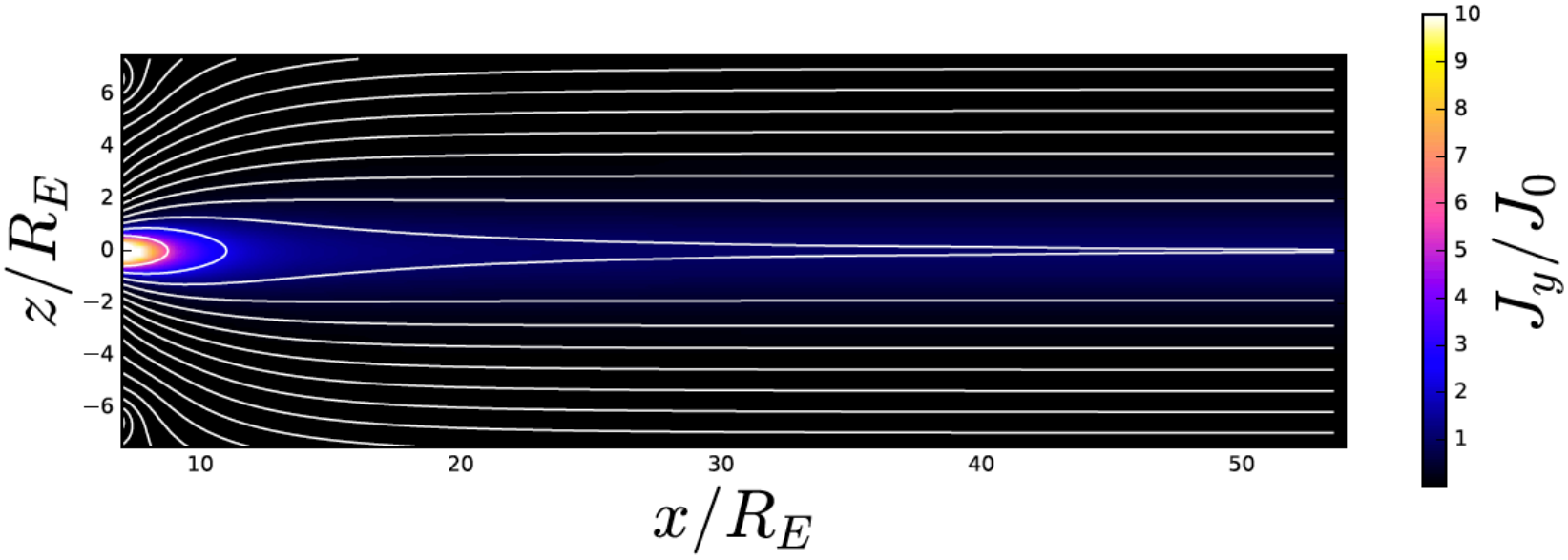

Exact kinetic equilibrium

(A.V. Manankova 2003)

$m_i/m_e Z = 25 \quad T_i/T_e = 5$

$R_E/d_i = 5 \quad \Delta_{sheet}/d_i = 10$

Two-dimensional simulation isolates the role of reconnection

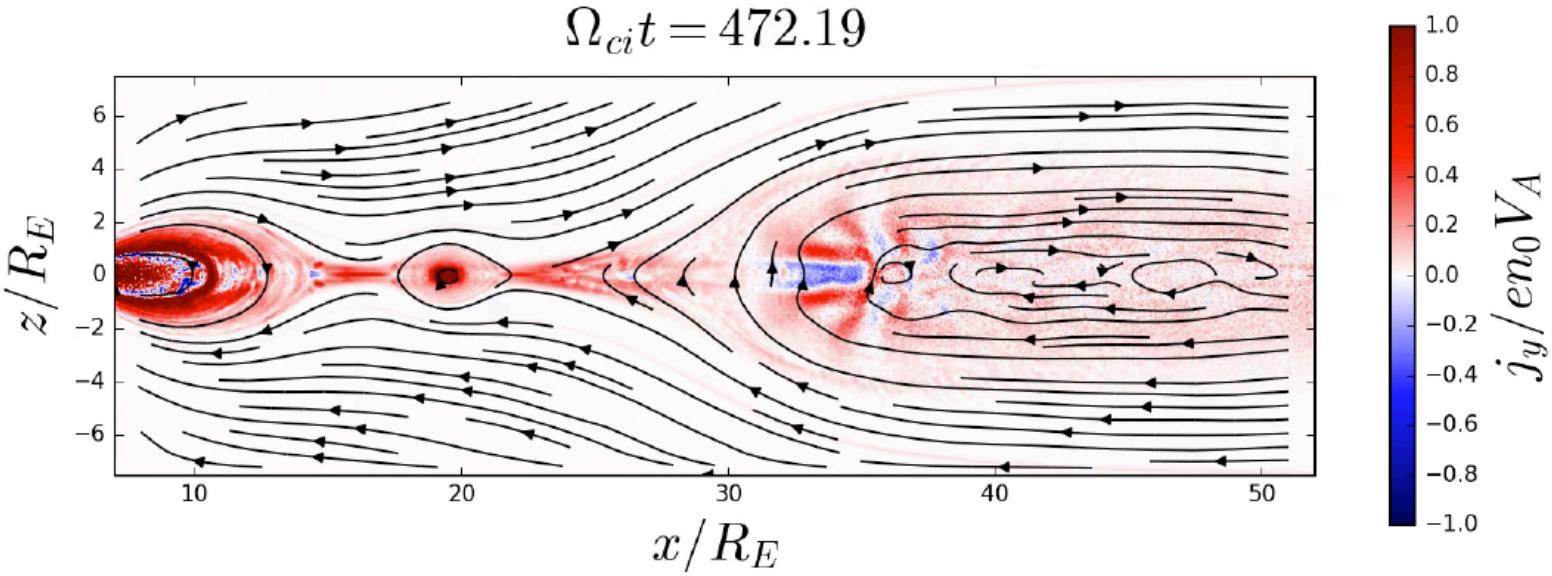

- Solar wind driving leads to thin current sheet formation and reconnection onset
- Reconnection drives Earthward and tailward plasma flows and produces plasmoids
- Dipolarization front is stable

Three dimensional simulation shows structure orthogonal to the reconnection plane

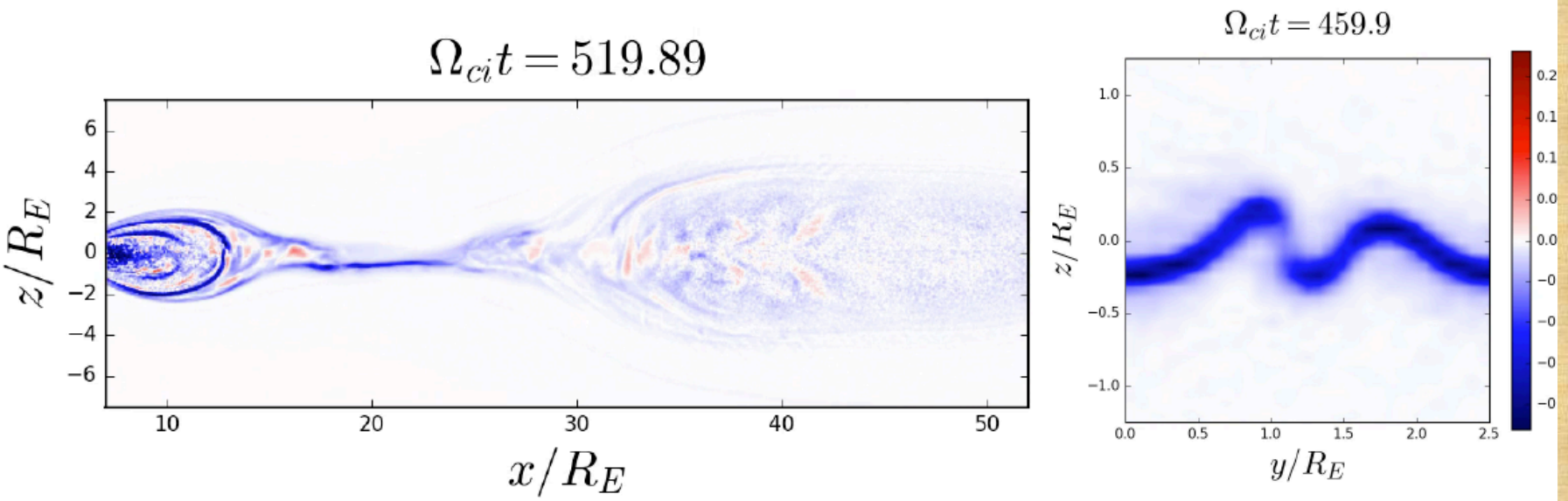

- Reconnection dynamics are qualitatively similar to the 2D case
- Current sheet flapping motions modulate the thin current sheet
- Dipolarization front becomes disrupted in the near-Earth region

Feld-aligned currents are produced and cross-tail current is disrupted

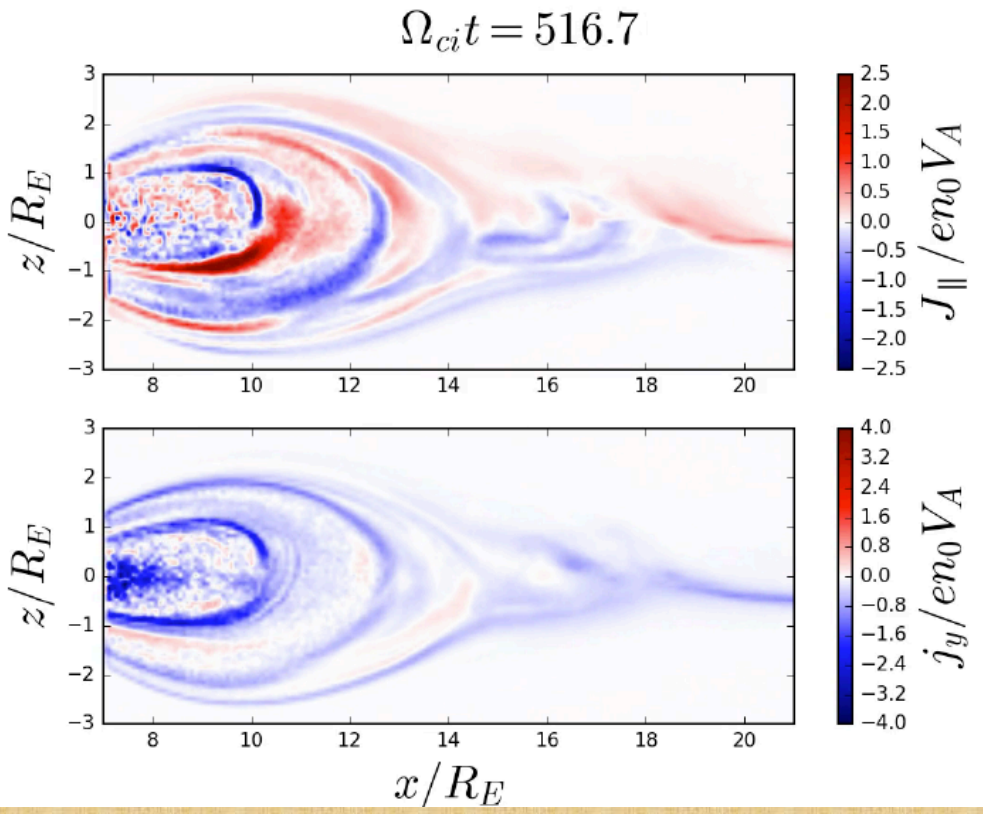

- Field-aligned currents travel to the ionosphere
- Cross-tail current shows a rapid disruption

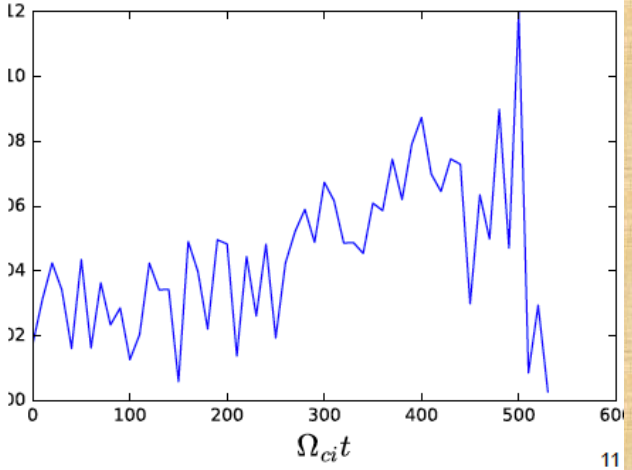

Energetic electrons and ions are produced in the disruption

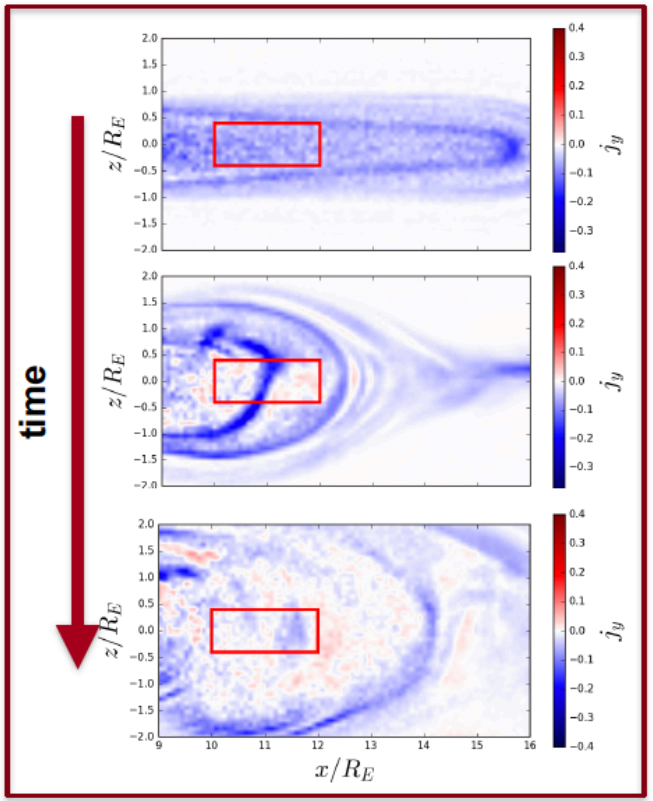

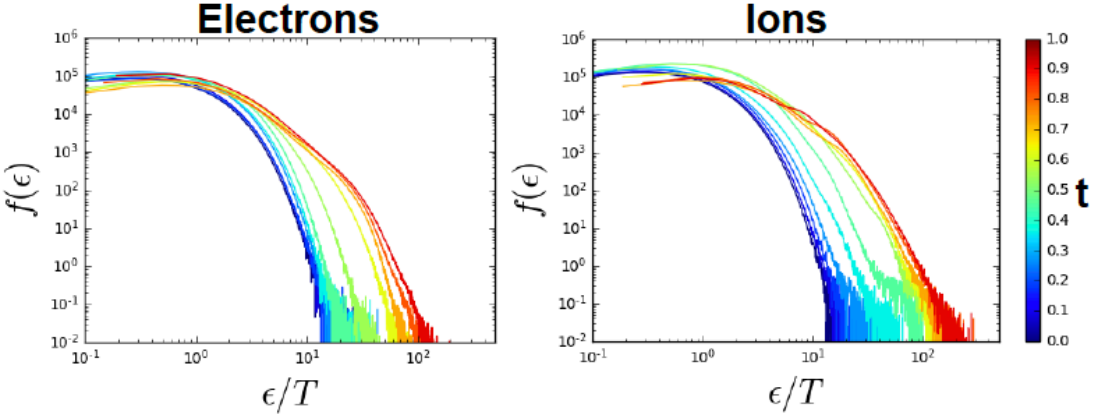

- Evolution of energy spectra for electrons and ions near Earth around the time of disruption
- Electrons and ions show significant acceleration to suprathermal energies

Key Regions of Magnetospheric Particle Acceleration

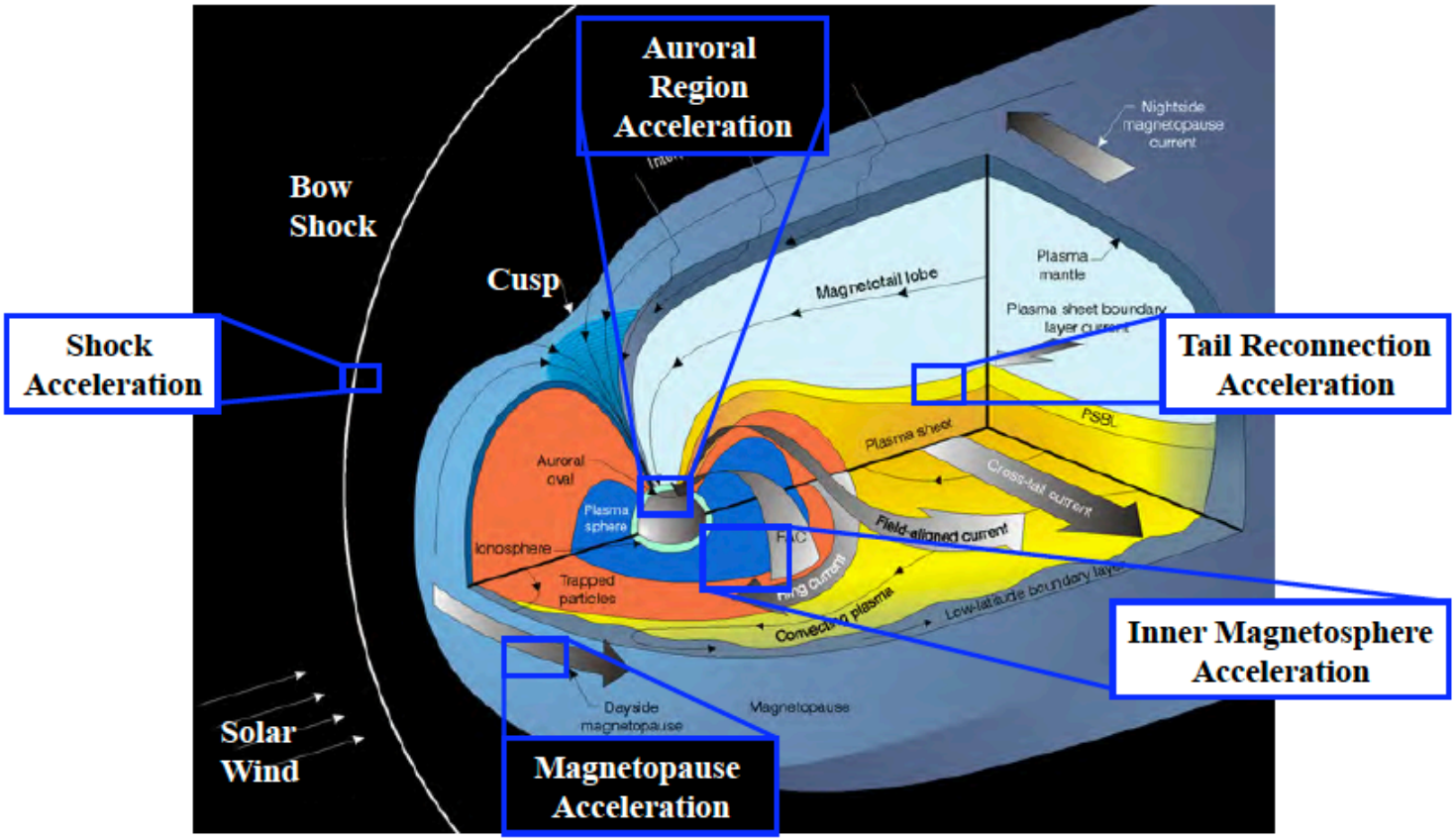

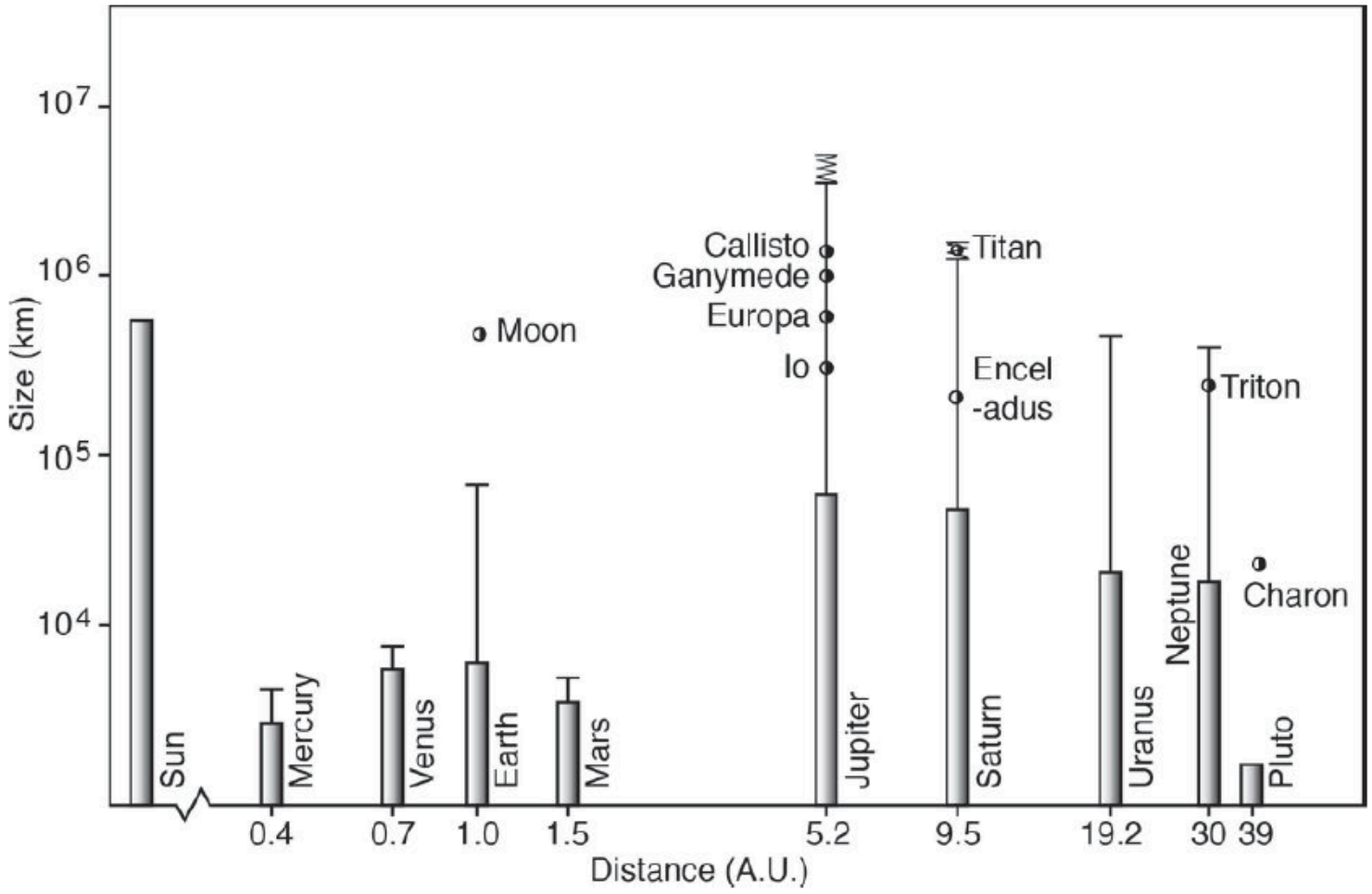
Size (km)
10^7
10^6
10^5
10^4
Sun
Mercury
Venus
Earth
Moon
Mars
Callisto
Ganymede
Europa
Io
Jupiter
Titan
Encel
-adus
Saturn
Uranus
Neptune
Triton
Charon
Pluto
0.4
0.7
1.0
1.5
5.2
9.5
19.2
30
39
Distance (A.U.)

Tilts and Obliquities

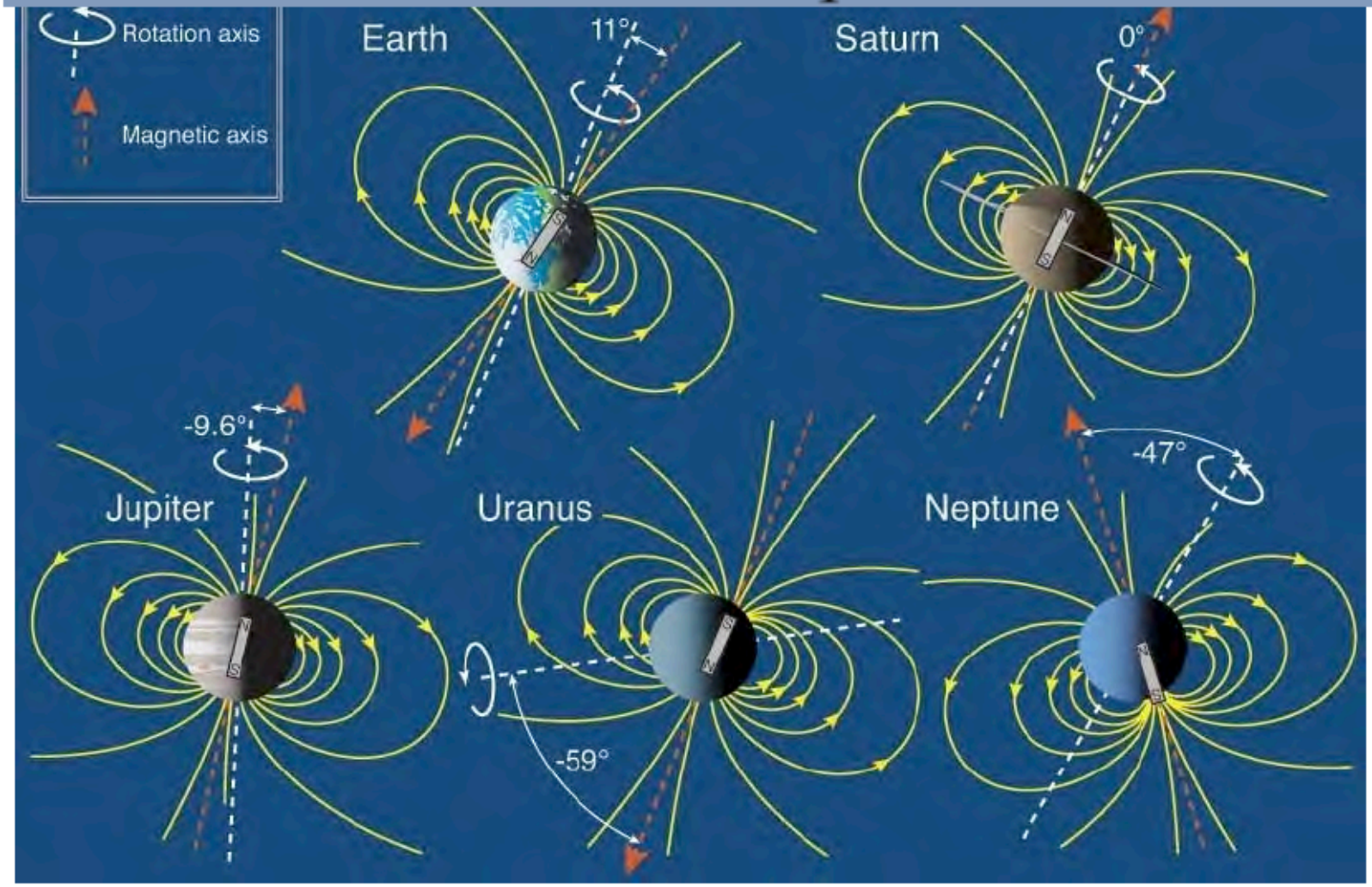

Offset Tilted Dipole (poor) Approximation

Dipole Magnetic Field in Solar Wind

SW Ram Pressure ⟷ Magnetic Pressure

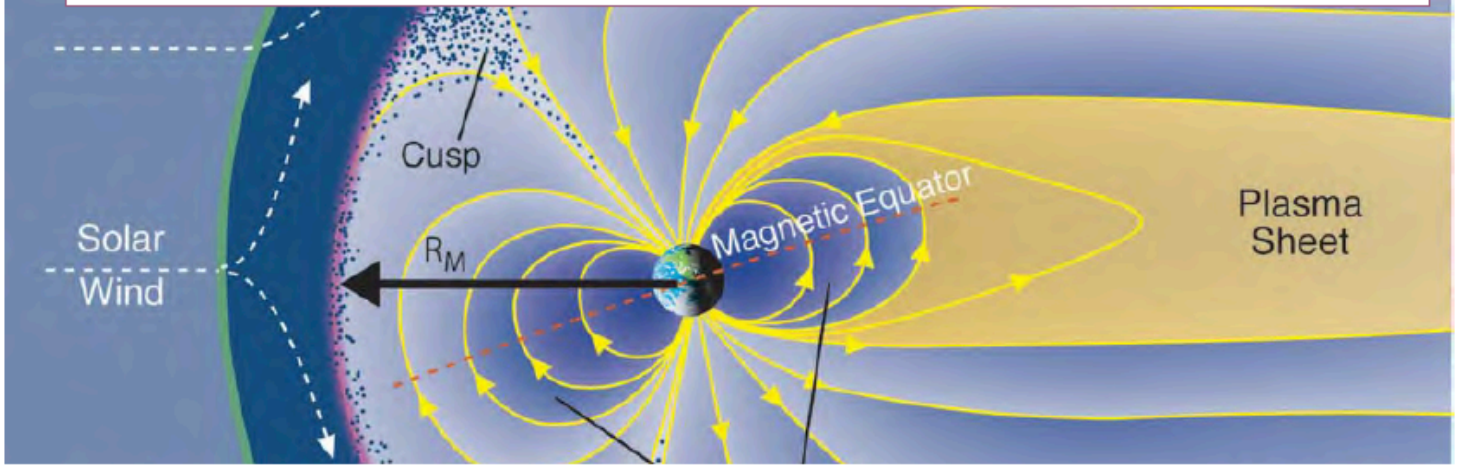

$$R_{MP} / R_{planet} \sim 1.2 \left[B_o^2 / 2 \mu_o \rho_{sw} V^2_{sw} \right]^{1/6}$$

Chapman-Ferraro Distance

$$R_{MP}/R_{planet} \sim 1.2 \{B_o^2 / 2 \mu_o \rho_{sw} V^2_{sw}\}^{1/6}$$

	Mercury	Earth	Jupiter	Saturn	Uranus	Neptune
B_o Gauss	.003	.31	4.28	.22	.23	.14
R_{MP} Calc.	1.4 R_M	10 R_E	46 R_J	20 R_S	25 R_U	24 R_N
R_M Obs.	1.4-1.6 R_M	8-12 R_E	63-92 R_J	22-27 R_S	18 R_U	23-26 R_N

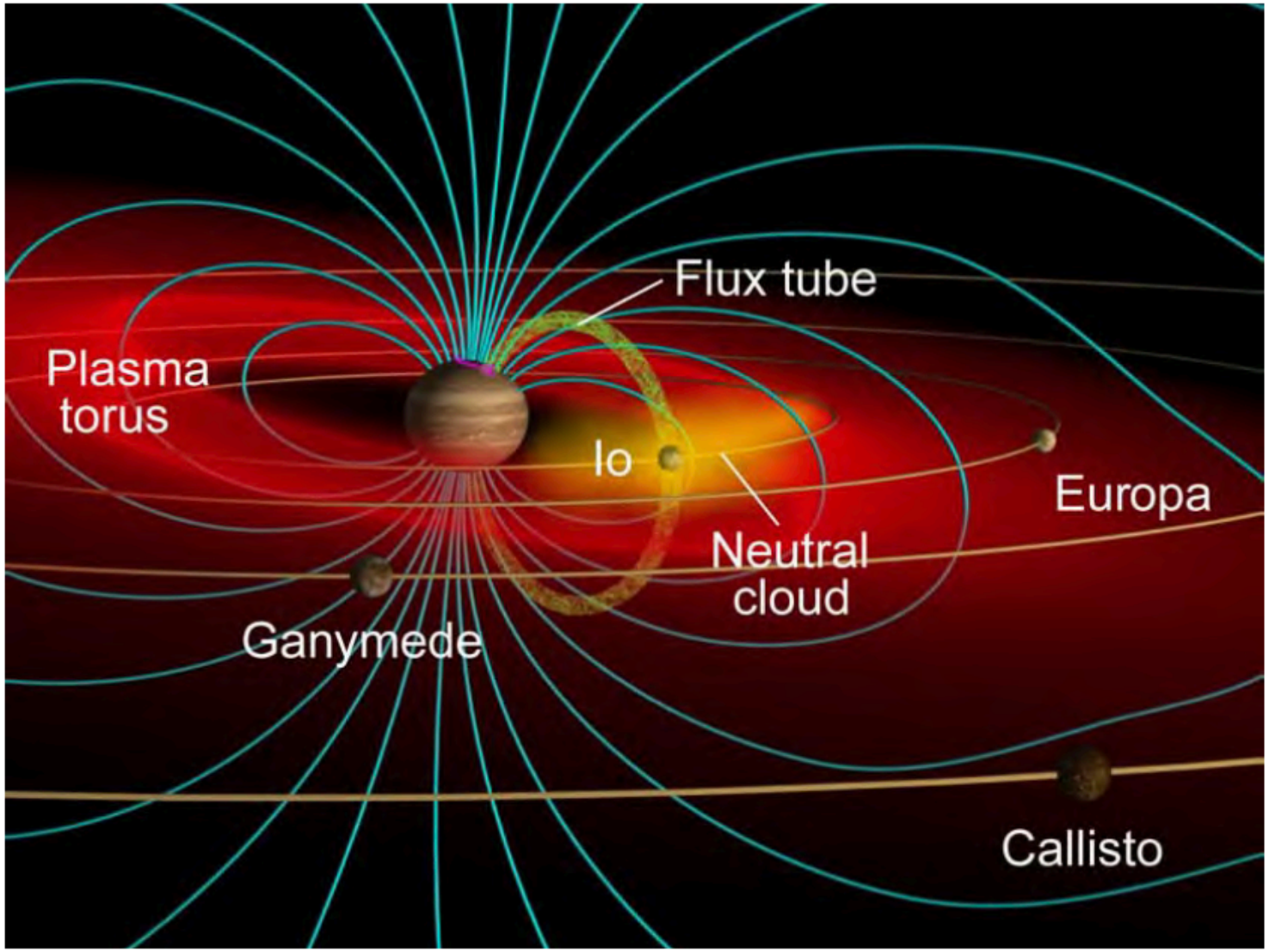
Flux tube
Plasma
torus
Io
Europa
Neutral
cloud
Ganymede
Callisto

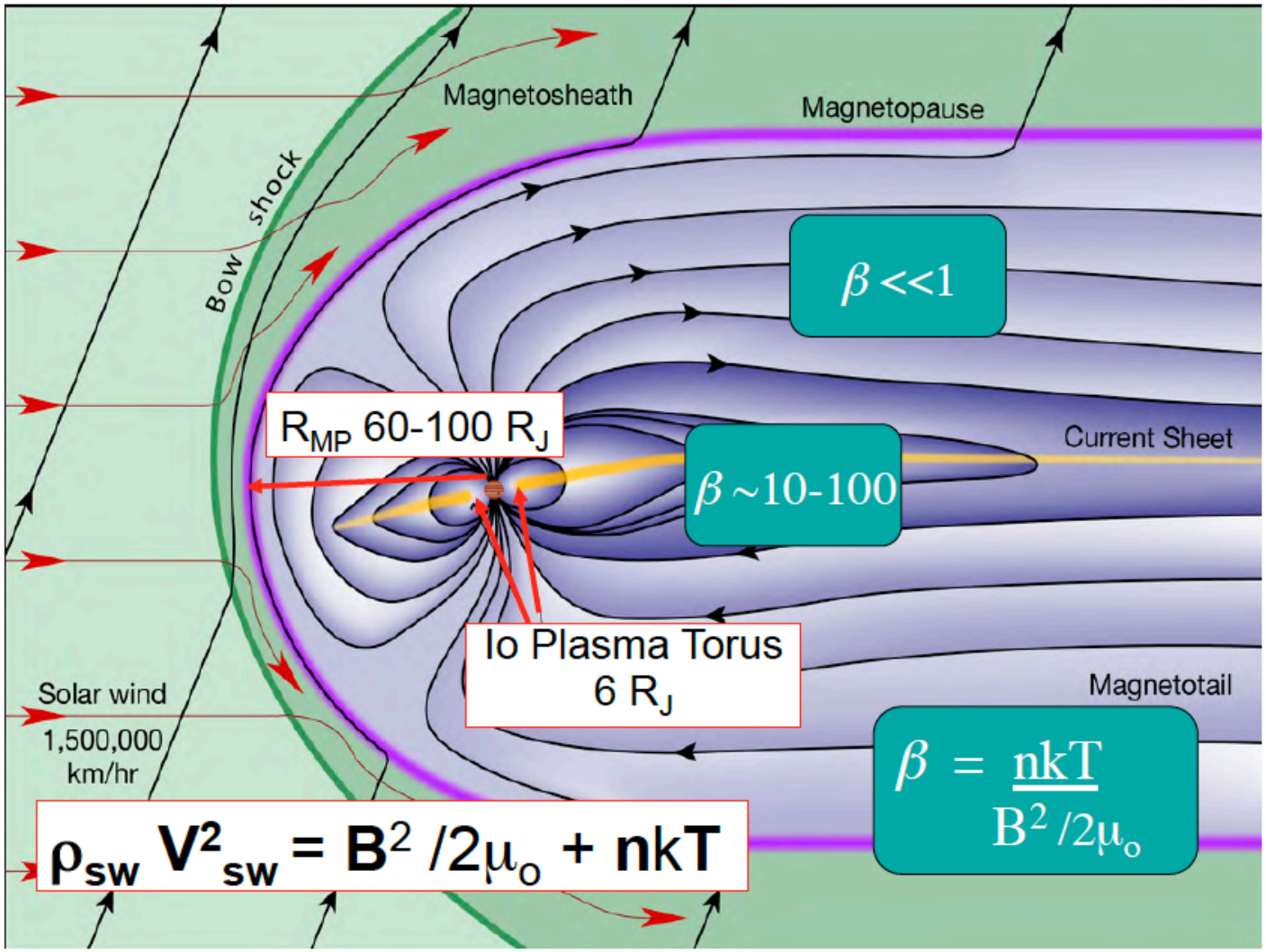
Magnetosheath
Magnetopause
Bow shock
β <<1
R_{MP} 60-100 R_J
Current Sheet
β ~10-100
Io Plasma Torus
6 R_J
Solar wind
1,500,000
km/hr
Magnetotail
$\beta = \frac{nkT}{B^2/2\mu_o}$
$\rho_{sw} V^2_{sw} = B^2/2\mu_o + nkT$

Plasma Sources

	Mercury	Earth	Jupiter	Saturn	Uranus	Neptune
N_{max} cm^{-3}	~1	1-4000	>3000	~100	~3	~2
Comp-osition	H^+ Solar Wind	O^+ H^+ Iono-sphere	O^{n+} S^{n+} Io	O^+ H_2O^+ H^+ Enceladus	H^+ Iono-sphere	H^+ N^+ Triton Iono-sphere
Source kg / s	?	5	700-1200	70-700	~0.02	~0.2

Aurora around Saturn & Jupiter

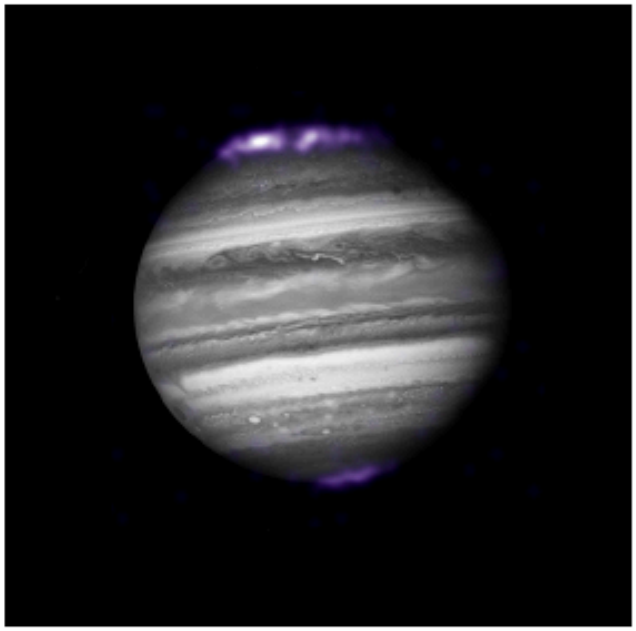

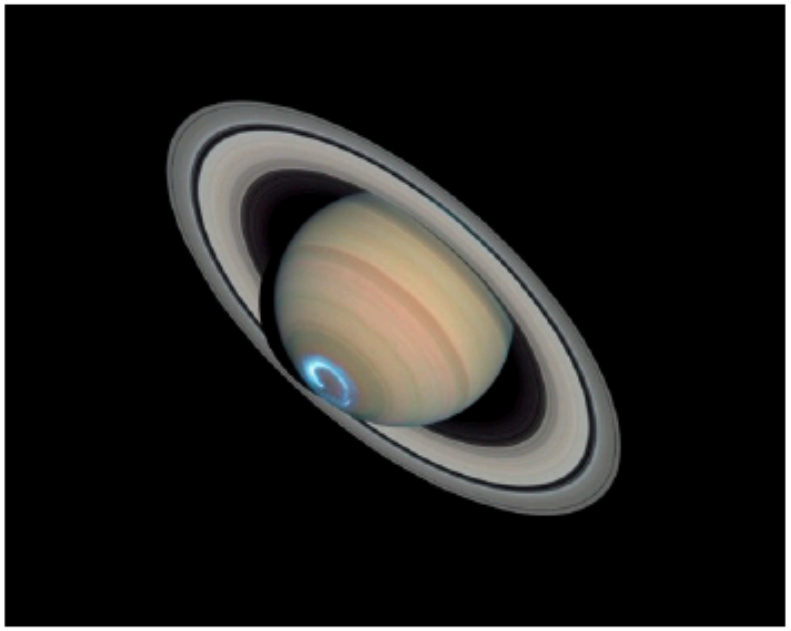

- Left: X-ray aurora observed by Chandra around Jupiter
- Right: UV aurora observed around Saturn
- Aurora recently observed in radio around brown dwarf
- Can observations of aurora help characterize the magnetic field and space environment of exoplanets?